

# Modification of Cast Al-Mg<sub>2</sub>Si Metal Matrix Composite by Li

R. HADIAN, M. EMAMY, and J. CAMPBELL

The effects of both Li modification and cooling rate on the microstructure and tensile properties of an *in-situ* prepared Al-15 pct Mg<sub>2</sub>Si composite were investigated. Adding 0.3 pct Li reduced the average size of Mg<sub>2</sub>Si primary particles from ~30 to ~6 μm. The effect of cooling rate was investigated by the use of a mold with different section thicknesses from 3 to 9 mm. The results show a refinement of primary particle size as a result of both Li additions and cooling rate increases, and their effects are additive. Similarly, both effects increased ultimate tensile stress (UTS) and elongation values. The thin sections show somewhat unexpectedly low and scattered tensile results attributed to the casting defects observed in fracture surfaces. The Li-modified alloy displays serrated yielding behavior that is not fully explained here. The refinement by Li and enhanced cooling rate is explained in terms of an analogy with the effect of Sr and cooling rate in Al-Si alloys, and is ultimately attributed to the effect of the alkali and alkaline earth metals deactivating oxide double films (bifilms) suspended in Al melts as favored substrates for intermetallics.

DOI: 10.1007/s11663-009-9251-1

© The Minerals, Metals & Materials Society and ASM International 2009

## I. INTRODUCTION

THE Al- and Mg-based composites, reinforced with particulates of Mg<sub>2</sub>Si, have been lately introduced as a new group of particulate metal matrix composites (PMMCs) that offer attractive advantages such as low density, good wear resistance, and good castability.<sup>[1,2]</sup> Al-Mg<sub>2</sub>Si hypereutectic alloys seem to be potential candidates to replace Al-Si alloys used in aerospace and engine applications. *In-situ* preparation of Al-Mg<sub>2</sub>Si composites seems to be the best way of fabricating such PMMCs, because advantages such as an even distribution of the reinforcing phase, good particle wetting, and low costs of production are guaranteed. There have been reports of Mg-Mg<sub>2</sub>Si composites made by mechanical alloying and hot extrusion methods in which the alloys show good tensile properties, but these manufacturing routes are expensive. Therefore, over the past few years, efforts have been made to produce such composites by a casting process. Despite the fact that Mg<sub>2</sub>Si intermetallic particles exhibit a high melting temperature, low density, high hardness, low thermal-expansion coefficient, and equilibrium interface, their coarse and rough morphology in the Al matrix has been thought to lead to the low ductility observed in these materials.<sup>[3]</sup>

Thus, investigations have been carried out to modify the primary and eutectic Mg<sub>2</sub>Si structure in an effort to improve the properties of these composites. Other than expensive methods of rapid solidification and mechanical alloying,<sup>[4]</sup> high cooling rates and impurity modifications are well-known techniques that have been used so far. Zhang *et al.*<sup>[5]</sup> used a wedge copper mold with a range of cooling rates, and Ourfali *et al.*<sup>[6]</sup> applied Bridgman solidification with different withdrawal velocities. Both methods were found to be effective in refining the coarse Mg<sub>2</sub>Si structure and producing a final dendritic structure. Dendrites, however, can result in anisotropic properties, and in order to improve tensile properties, a more isotropic microstructure is preferred. Other efforts have been focused on the modification of the structure with addition of different alloying elements such as Sr, Ce, sodium salt (assumed to introduce Na), K<sub>2</sub>TiF<sub>6</sub>, and extra silicon content.<sup>[7-11]</sup> Rare earth elements have also been reported to be capable of modifying the primary Mg<sub>2</sub>Si particles.<sup>[12]</sup> Recently, P was added to the composite and the results show a great change in size and morphology of primary particles and a transition from flakes to fibers in the eutectic structure.<sup>[13]</sup>

Assuming an analogy with the modification of Al-Si alloys by such elements as Na and Sr, a refinement of the microstructure is expected to result in an improvement of the mechanical properties. The influence of particle size on the mechanical properties of MMCs has been investigated<sup>[14]</sup> and the results confirm the expectation that the finer the particle size, the higher the strength. So far the finest size of primary Mg<sub>2</sub>Si particle reported in the literature is about 8 μm.<sup>[12]</sup>

The objective of the present study is to evaluate the tensile properties of Al-15 pct Mg<sub>2</sub>Si composites and fracture characteristics of the material with the addition of up to 0.3 pct Li.

---

R. HADIAN, Doctoral Student, is with McMaster University, Hamilton L8S 4L8, Canada. Contact e-mail: hadianra@mcmaster.ca  
M. EMAMY, Professor, is with the School of Metallurgy and Materials, University of Tehran, Tehran, Iran. J. CAMPBELL, Emeritus Professor, is with the Department of Metallurgy and Materials, University of Birmingham, Birmingham B15 2TT, United Kingdom.

This article is based on a presentation given in the "3rd Shape Casting Symposium," which occurred during the TMS Spring Meeting in San Francisco, CA, February 15-19, 2009, under the auspices of TMS, the TMS Light Metals Division, the TMS Solidification Committee, and the TMS Aluminum Processing Committee.

Article published online June 24, 2009.

A relatively new factor, until recently commonly overlooked, but which has been introduced into the discussion of this work, is the probable presence of doubled-over oxide films that will be in suspension in the alloy. These defects can occur in huge numbers by the folding-in of the oxide skin of the melt during the turbulence generated during the pouring of a casting. Because the film naturally folds dry side to dry side, and so experiences no bonding across these surfaces, this doubled-over interface forms an effective crack in the liquid. The crack can be frozen into the solid, reducing its mechanical properties. The outer faces of the double film are, of course, in perfect atomic contact with the melt and have been shown to act as substrates for the nucleation and growth of intermetallics in a wide variety of alloy systems. The reason that bifilms, although nearly always present in castings, have been generally overlooked, is because they are so thin, often only a few nanometers in thickness. Dense populations of bifilms seem to be present in most Al alloys, and remain in suspension in light alloy melts for long periods because of their near-neutral buoyancy. Summaries of bifilm defects and their behavior can be seen in a number of reviews.<sup>[15,16]</sup> The results of this work therefore have been explained assuming oxide bifilms to be present.

## II. EXPERIMENTAL

Industrially pure elemental Al, Mg, and Si were used as starting materials to prepare Al-15 pct Mg<sub>2</sub>Si composite. All the materials were preheated at 200 °C and were melted in an electrical resistance furnace using a 10-kg SiC crucible. The chemical composition of hyper-eutectic Al-15 pct Mg<sub>2</sub>Si determined by optical spectrograph was Al-5.5Si-9.7Mg-0.09Fe-0.001Cu-0.02Mn-0.003Cr-0.007Ni-0.004Zn-0.009Ti (all in wt pct). This parent alloy was remelted in order to prepare alloys with 0, 0.1, and 0.3 wt pct Li. When the temperature reached 750 °C, pure Li was wrapped in aluminum foil and added in small increments, with continual addition of a protective flux powder to ensure that the melt surface remained covered. In spite of this precaution, it was found necessary to add 20 pct additional Li to ensure that the Li target composition was reached. In the absence of argon, degassing was conducted by using dry C<sub>2</sub>Cl<sub>6</sub> powders with a purity of 99.9 pct. C<sub>2</sub>Cl<sub>6</sub> powders of 0.3 wt pct of the molten alloy were wrapped in aluminum foil before submerging into the melt using a stainless steel plunger. Steel tools were coated with a ceramic wash to reduce contamination of the melt. The melt was degassed for 5 minutes. Facilities were not available for checking the oxide or hydrogen contents of the melt.

After stirring and cleaning off the dross, alloys with different compositions were top-poured into cylindrical ingot molds (30-mm diameter and 60-mm height) that were used for microstructural studies. Specimens were cut from a standard location 25 mm from the base of the ingots.

To evaluate the effects of both cooling rate and Li modification on tensile properties, test bar castings

varying in thickness from 3 to 9 mm were poured in a sand mold (Figure 1). An open cylinder acted as both the pouring basin and the sprue and featured a ceramic foam filter directly at its base as in a so-called direct pour system.<sup>[17]</sup> The low sprue height of only 31 mm and low subsequent fall height after the filter (15 mm) were selected to reduce entrainment defects and enhance reproducibility of the results.<sup>[17]</sup> The cooling rates in the bars were estimated to be approximately in the range 10 to 100 Ks<sup>-1</sup> for the 9- and 3-mm sections, respectively.

The cooling rate in the 30-mm-diameter ingots used to check microstructure was somewhat slower than that in the 9-mm sand sections, but the difference was minimal as a result of (1) the radial symmetry of cooling in the larger casting, encouraging faster heat loss; and (2) the increased conductivity of the cast iron mold vs the silica sand mold. Thus, the microstructures of the ingots were reasonably representative of the structures in the test bars. Any small difference was insignificant compared to the substantial observed effect of Li on the microstructures.

Tensile test bars were machined, according to ASTM-B577<sup>[18]</sup> flat subsize specimens, to 25-mm gage length, 6-mm width, and 3-mm thickness for each condition. The material was not heat treated. The tensile tests were carried out on a computer-controlled MTS tensile testing machine, equipped with a strain gage extensometer, at a constant crosshead speed of 1 mm/min (corresponding closely to  $6.6 \times 10^{-4}$  s<sup>-1</sup> since necking was insignificant).

Specimens for microstructural characterization were sectioned from the gage length portion of the test bars. Metallographic specimens were polished and etched by HF (1 pct). To remove the Al matrix, specimens were deeply etched in 15 pct NaOH solution. Quantitative data on microstructure were determined using an optical microscope equipped with an image analysis system (Clemex Vision Pro Version 3.5.025). The microstructure was examined by scanning electron microscopy (SEM) performed in a VEGA\* Tescan scanning electron

---

\*VEGA is a trademark of Tescan, Brno, Czech Republic.

---

microscope operated at 15 kV with energy-dispersive X-ray analysis.

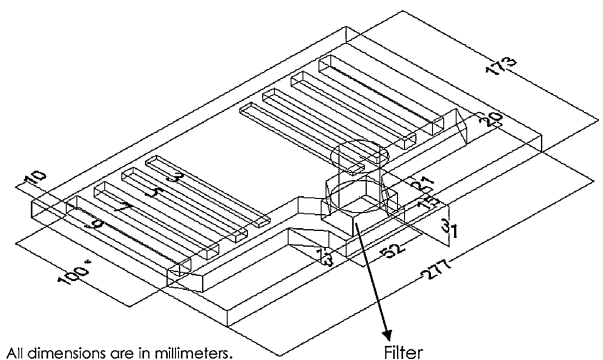


Fig. 1—Schematic image of sand cast tensile test bars.

### III. RESULTS AND DISCUSSION

Figures 2 and 3 show typical microstructures of Al-15 pct Mg<sub>2</sub>Si as-cast alloy (a) before and (b) after refinement with Li. Addition of 0.3 pct Li has been proved to modify the microstructure more effectively. According to the schematic phase diagram (Figure 4),<sup>[19]</sup> since the alloy has a hypereutectic composition, the microstructure should contain dark faceted primary particles of Mg<sub>2</sub>Si in a matrix of Al-Mg<sub>2</sub>Si eutectic. The fact that also clearly seen are bright primary  $\alpha$ -Al grains indicates that undercooling has occurred, allowing both primary phases to form together with the eutectic in the form of a matrix of well-developed Al-Mg<sub>2</sub>Si eutectic cells (or eutectic grains according Kurz and Fisher<sup>[20]</sup>). The existence of the two primary phases (primary  $\alpha$ -Al

and primary Mg<sub>2</sub>Si) is the result of the nonequilibrium solidification of the alloy in which the primary phases can grow alongside the eutectic in the coupled zone below the equilibrium eutectic temperature.

Our main interest in the MMC structure centers on the mean size of Mg<sub>2</sub>Si particles. Here, in the unmodified 9-mm section, it is about 30  $\mu$ m. The coarse Mg<sub>2</sub>Si primary crystals in an unmodified alloy often grow as hollow shapes (Figure 2(a)) similar to coarse primary silicon in the Al-Si system.<sup>[21]</sup> These hopper crystals are not seen in the finer Mg<sub>2</sub>Si particles in Li-modified alloys. Addition of Li up to 0.3 pct reduces their size to  $\sim$ 6  $\mu$ m and forms an even distribution of particles in the matrix. In addition to refinement of size, the morphology of the particles changes from faceted to a more

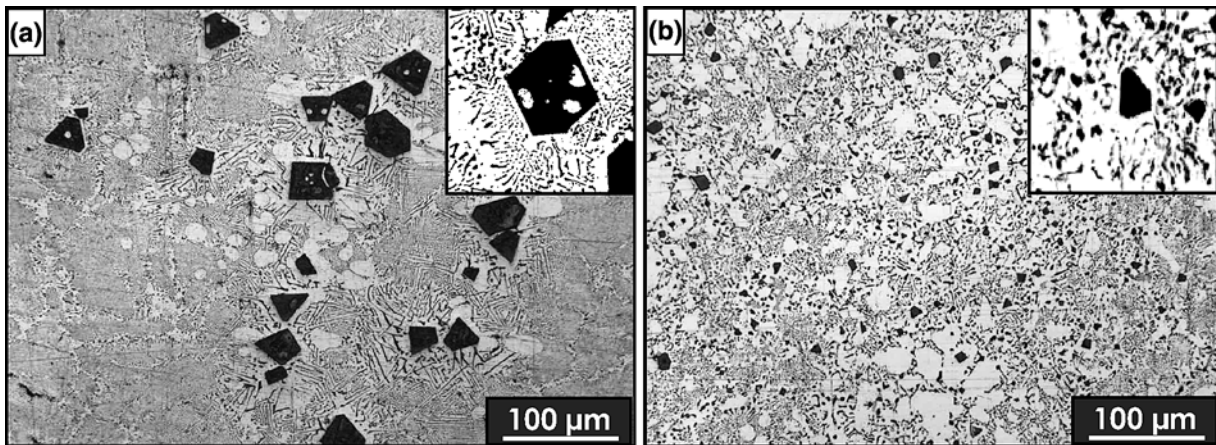


Fig. 2—(a) Typical microstructure of permanent mold Al-15 pct Mg<sub>2</sub>Si. (b) Microstructure after modification with 0.3 pct Li.

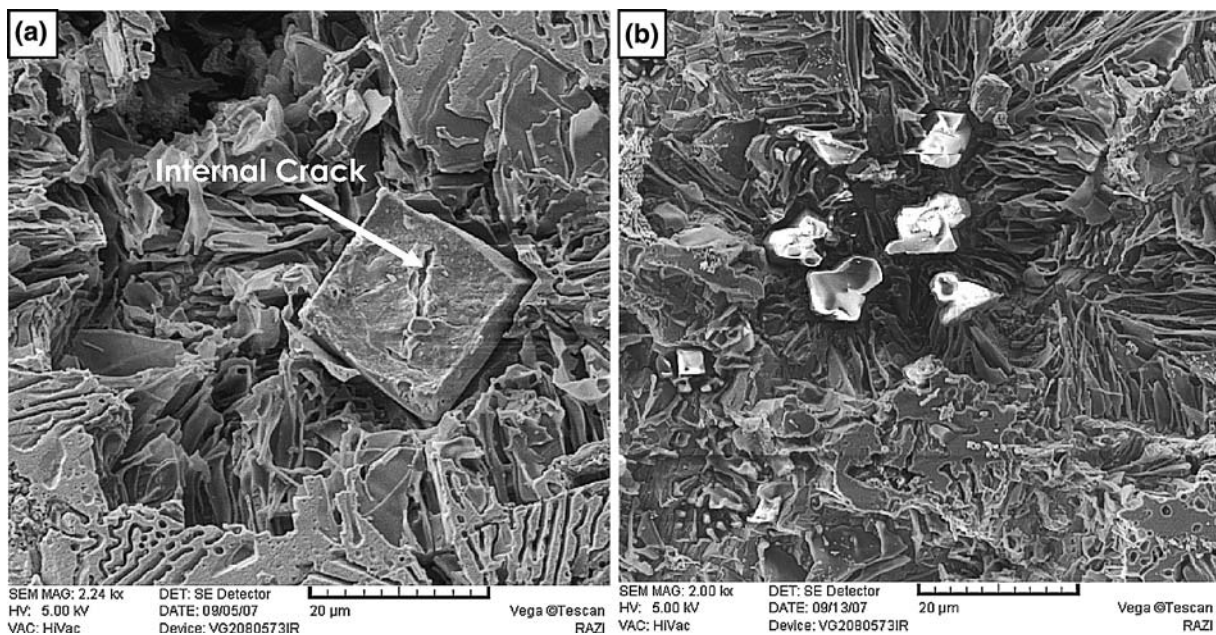


Fig. 3—(a) SEM micrograph of a primary Mg<sub>2</sub>Si particle surrounded by eutectic flakes in an unmodified alloy. (b) Primary Mg<sub>2</sub>Si particles surrounded by a fibrous eutectic structure in the Li-modified alloy. Both samples were deeply etched to remove the aluminum matrix.

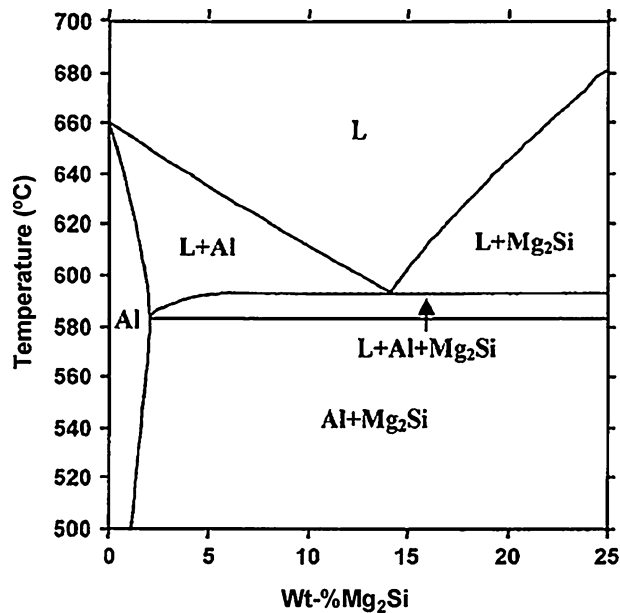


Fig. 4—Pseudo-binary phase diagram for Al-Mg<sub>2</sub>Si.<sup>[18]</sup>

smooth and rounded form (Figures 2(b) and 3(b)). A change in surface energy of Mg<sub>2</sub>Si crystals caused by Li atoms on its surface or in solution in its lattice may be responsible for the change in growth pattern.<sup>[22]</sup>

The refinement in size of the Mg<sub>2</sub>Si intermetallics could be the result of two major possibilities: (1) there may be a contribution from a genuine intrinsic factor explicable by traditional physical metallurgy; but (2) it seems certain that there is also a key contribution arising from process metallurgy and extrinsic factors (the presence of oxide bifilms in the melt). The input of processing to the development of microstructures is a relatively recent concept. Both these possibilities are described briefly as follows.

(1) Conventional physical metallurgical thinking might attribute the microstructural refinement to a change in phase diagram due to high constitutional undercooling. There is also a possibility that Li might have shifted the eutectic point toward the Mg<sub>2</sub>Si-rich side of the phase diagram. Further observations of Figure 2(b) show that the volume fraction of  $\alpha$ -Al was increased with increasing Li content, but the eutectic cell area was appreciably reduced. The Li could achieve this by intensifying the skewed coupled zone in the Al-Mg<sub>2</sub>Si binary diagram. Also, larger  $\alpha$  grains may be a consequence of a wider ternary range in the diagram.<sup>[22]</sup> As clearly seen in the magnified sections of Figures 2(a) and (b), in the unmodified structure, the pseudo-eutectic structure is mainly fibrous inside the cells, corresponding to a high rate of freezing, but a lamellar structure is observed at the cell boundaries. With the addition of Li, the eutectic at the cell boundaries changes from a flake morphology to a structure in which some of the Mg<sub>2</sub>Si eutectic particles are approximately of the same size as the refined primary Mg<sub>2</sub>Si particles. This coarsening of structure in the intercellular

regions is likely to be the result of some Li segregation and the accompanying reduction in interfacial energy of the intermetallic.

(2) Turning now to the possibility of the influence of process metallurgy, in common with many other alloy systems, there is increasing evidence that the intermetallics nucleate and grow on oxide bifilms suspended in the melt.<sup>[16]</sup> The analogy with the precipitation of primary Si in Al-Si alloys appears almost exact: the primary Si normally precipitates on oxides in the melt, straightening the oxides from their normally convoluted and raveled forms as the crystal grows, thus straightening the crack in the center of the oxide. The straightened and thus more effective crack thereby reduces properties.<sup>[16]</sup> When Sr is added, the Sr appears to deactivate the favored status of the oxide, possibly by coating and blocking growth sites on the oxide. The Si is then prevented from precipitating as a primary phase and is forced to nucleate at a lower temperature on less favorable substrate(s) after which it grows as a eutectic. We call this structure a “modified” structure. The reduced formation temperature of the eutectic Si is a characteristic feature of Si modification.<sup>[23]</sup>

The action of Li in the present MMC appears to be similar. In the absence of Li, the intermetallics precipitate on and straighten bifilm cracks and so degrade properties, but in the presence of Li, the oxide is prevented from acting as a substrate. Easy nucleation is now prevented, forcing the growth of the intermetallic as a lower temperature eutectic phase. The bifilm defects then remain in their convoluted, compact morphology in which they are relatively harmless as cracks, so that the properties of the casting are improved. Interestingly, however, in contrast with the action of Sr in Al-Si alloys, the transformation of the intermetallic is not complete in this alloy, so that some small primary phases remain after the addition of Li. This finding raises the question whether sufficient Li was added to complete the transformation, or whether the Li is simply somewhat less effective in this alloy. Future work will be required to clarify this.

The similar refinement of the intermetallics by the increase of freezing rate appears explicable because of the general rule that faster cooling results in higher undercoolings, which subsequently leads to more prolific nucleation and faster growth rates, and of course a more limited time for growth, finally yielding a finer microstructure (Figures 5 and 6). Figure 7 nicely illustrates the refinement of primary Mg<sub>2</sub>Si particle size in unmodified sections corresponding to faster freezing. (However, in Figure 7, the particle size in 9-mm sections appears somewhat smaller than expected, and if valid, is not understood.) It might be the result of some flotation of particles in the larger section, giving warning of the potential for gravity segregation of particles in larger sections.

In addition to these clear and fundamental physical reasons for the action of more rapid freezing, there is expected to be a further effect from process metallurgy that the bifilm introduces. The bifilm arrives in the casting in a crumpled, convoluted morphology because

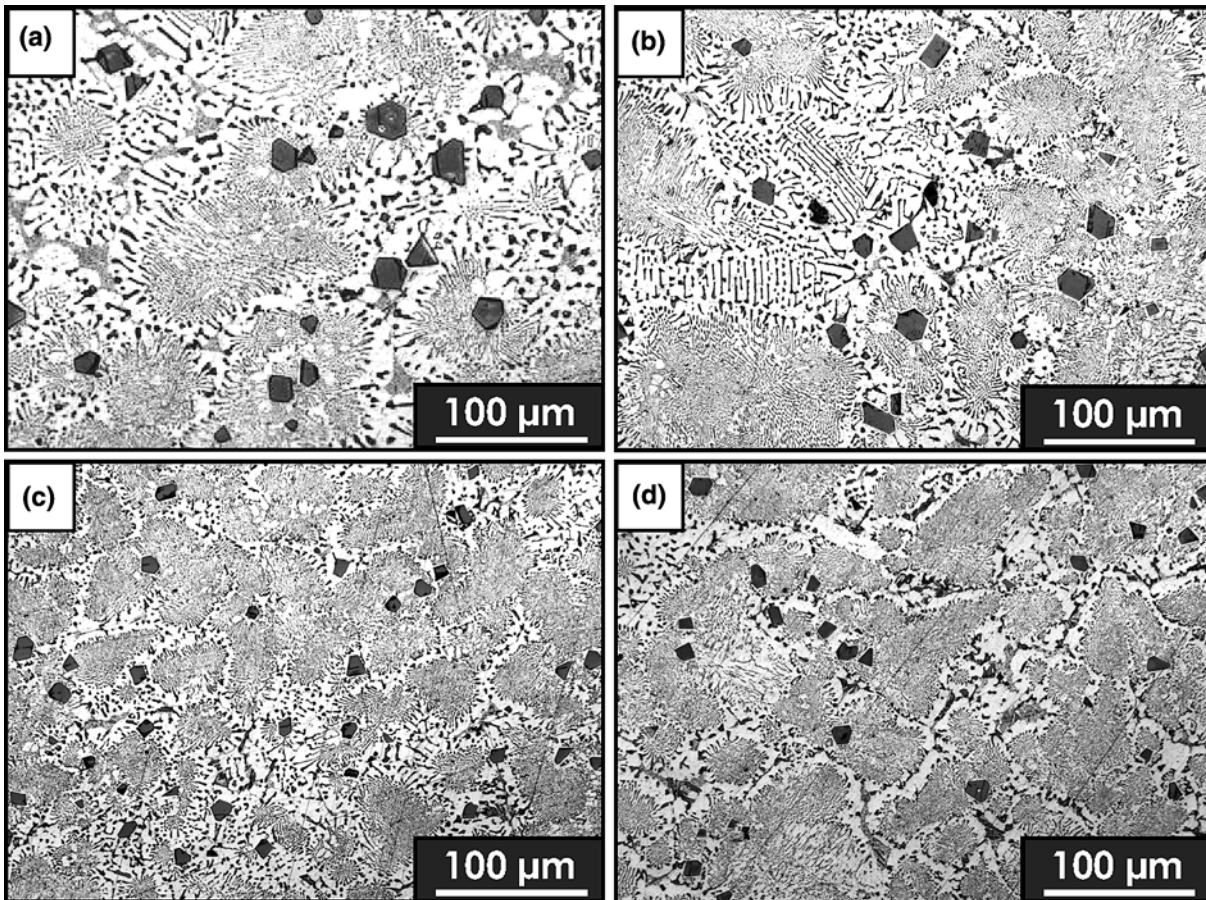


Fig. 5—Effect of cooling rate on microstructure of Al-15 pct Mg<sub>2</sub>Si without Li modification: (a) 9-mm, (b) 7-mm, (c) 5-mm, and (d) 3-mm sections.

of the action of turbulence during the filling of the mold. The crystal advances in a more or less directional manner over the surface of the bifilm, but its advance will be arrested at each crinkle and fold. The rate of unfurling (the opening out of the bifilm into a more or less flat sheet) will effectively control the rate of growth of the crystal as it advances from one fold to the next. The unfurling action occurs roughly a fold at a time against the viscous restraint of the liquid; the straightening of each fold has been predicted to a time measured in seconds or minutes, depending on the geometry of the bifilm and melt conditions.<sup>[15,16]</sup>

The improvement in properties by Li addition and by faster freezing can be attributed to the shorter intermetallic particles, whose shorter lengths have had limited straightening effect on their substrate oxide bifilms (each of which, it is necessary to recall, contains a central crack). Thus, the population of cracks in the liquid is only fractionally opened, the majority of bifilms remaining crumpled and compact, and so is relatively harmless. Properties will be higher for this population of shorter cracks.

The ultimate tensile strength (UTS) and elongation values of the specimens are plotted in Figures 8(a) and (b) as a function of test bar thickness. It is evident that both Li modification and faster freezing raise the tensile

strength of the unmodified alloy. Over the ranges of Li and freezing rate used in this work, Li is somewhat more effective, although not so much that could not be envisaged to be reversed in more favorable freezing conditions, such as might occur in metal molds, for instance. Thus, the chemical and freezing rate modifications are of a similar magnitude and are seen to be additive.

The results generally confirm expectations based on the metallographic results. Some scatter is observed in the results within each section, especially in elongation values. As is well understood, ductility is highly sensitive to the presence of defects in the alloy, particularly in this case, the presence of cracks opened to varying degrees by the precipitation, and growth of intermetallic crystals on bifilms. The scatter is most notably seen in 3-mm sections in both modified and unmodified samples. In addition, the 3-mm results are an exception to the observed trend of improved properties with reducing casting section thicknesses. It seems reasonable to attribute the variability in thinner sections to additional casting defects, which are exaggerated in thin wall castings, since any given defect will occupy a greater proportion of the thickness of the sample. Because of the relatively poor casting conditions, the entrainment of occasional air bubbles and more severe oxide bifilms

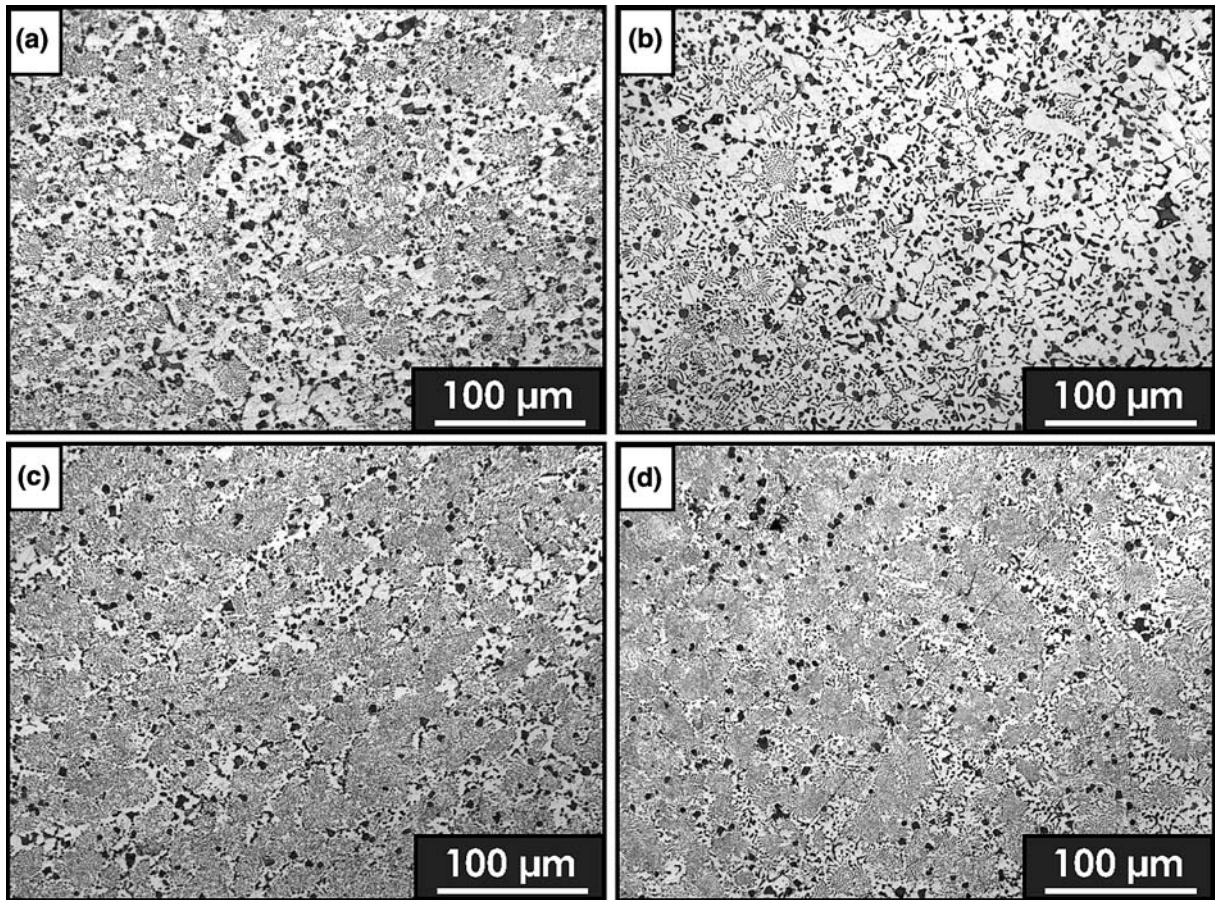


Fig. 6—Effect of cooling rate on microstructure of Al-15 pct Mg<sub>2</sub>Si with 0.3 pct Li modification. (a) 9-mm, (b) 7-mm, (c) 5-mm, and (d) 3-mm sections.

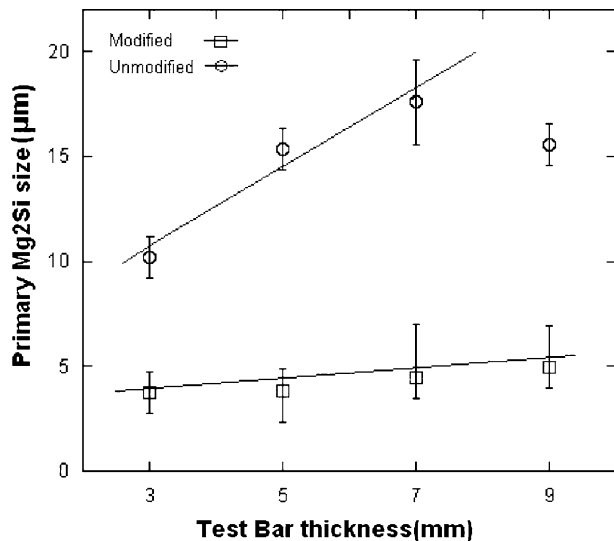


Fig. 7—Primary Mg<sub>2</sub>Si size vs section thickness.

is to be expected and explains the defects seen in Figures 9(a) and (b). For the future, improved casting techniques will refine the preliminary results presented here. In the meantime, the tentative extrapolations

noted in Figure 8 indicate truly impressive potential, with the possibility to achieve elongations well above 10 pct, which remains an incentive for future effort.

Occasional high tensile results from this experiment show that in specimens with lower defect contents, deformation continues until the expected fracture stress is reached. The presence of other macroscopic casting defects, such as shrinkage and air bubbles, implies that improving the casting process, in addition to microstructural modification, is required to obtain the highest elongation and UTS values attainable from these alloys.

The highest elongation value of 2.6 pct in this work was achieved in a modified 5-mm section. Compared to previous ductility data,<sup>[24]</sup> the current results indicate relatively low values. This discrepancy is probably the result of a different quality of material, or different melt preparation and casting procedures that have resulted in a different population of bifilms. The internal consistency of the current work seems nevertheless to be reliable.

An Mg<sub>2</sub>Si particle in Figure 10 is seen to be peeled open from what appears to be a central plane of weakness. It has not fractured into pieces, but has been deformed into a highly curved shape, clearly revealing that the Mg<sub>2</sub>Si phase is not brittle. Brittleness has often been assumed from the presence of cracks, but the

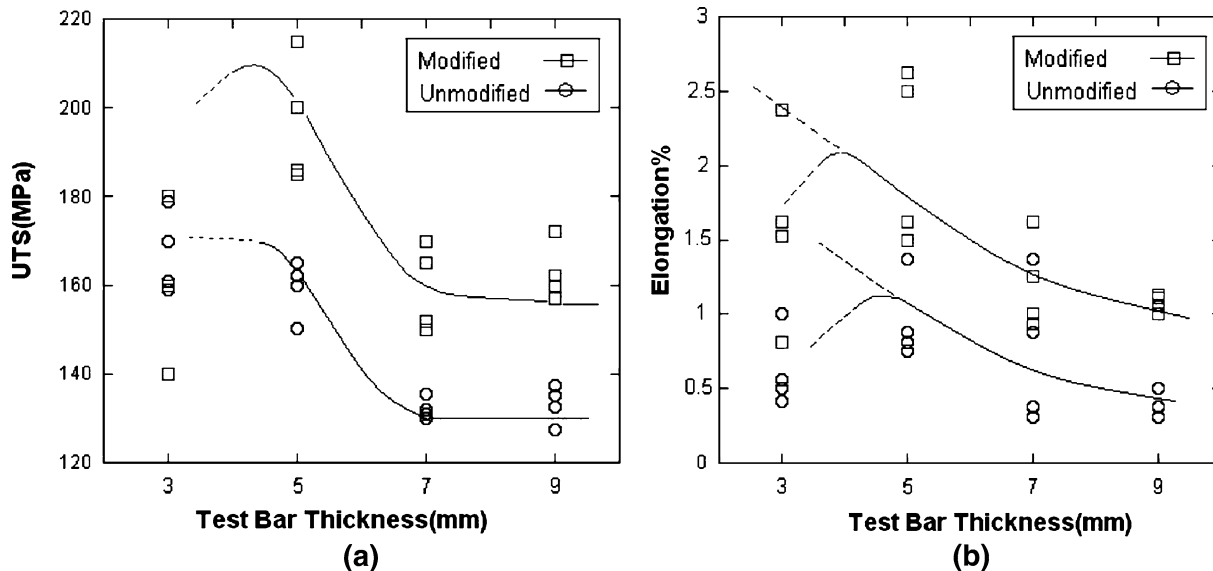


Fig. 8—Tensile properties as a function of test bar thickness: (a) UTS and (b) elongation.

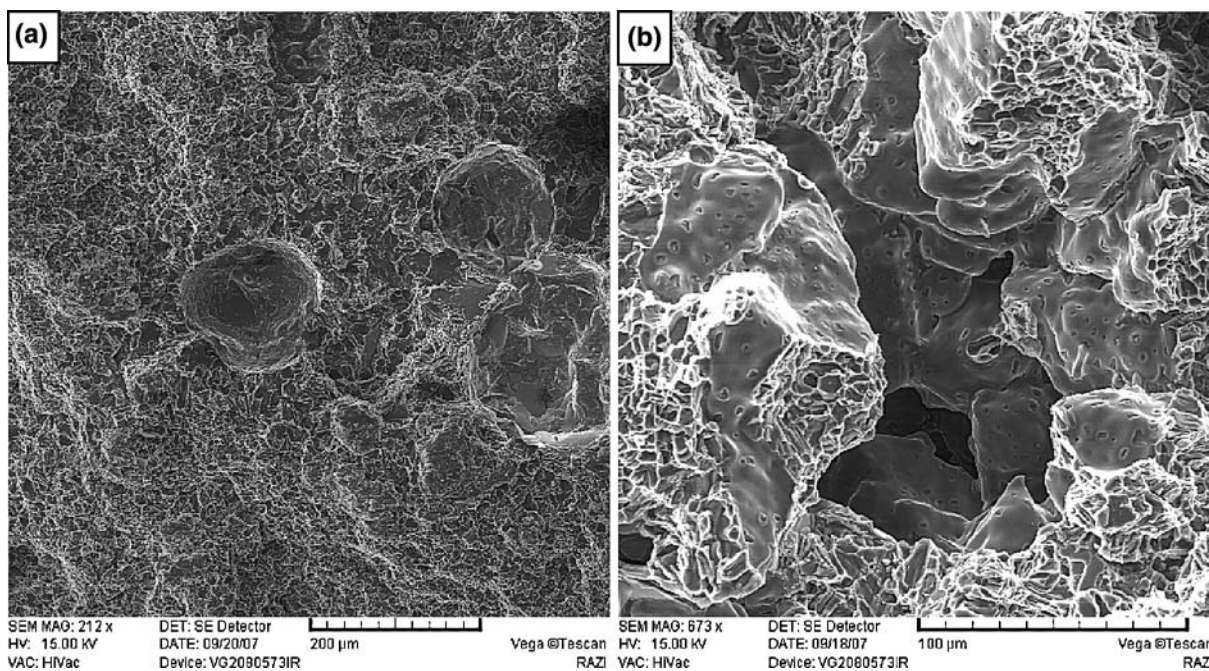


Fig. 9—(a) Gas porosity in a Li-modified 3-mm section and (b) shrinkage porosity in an unmodified 9-mm section.

cracks are a “foreign import” into the particle, an integral feature unfortunately introduced as a direct consequence of the presence of a crack in their favored substrates. We can conclude that the  $Mg_2Si$  particles are not only intrinsically hard, but also ductile if not weakened by the presence of their precracked substrates. Furthermore, the appearance of the intermetallics on the fracture surfaces, most of which are seen to contain a single central crack (Figure 11), is directly explained by the bifilm concept.

Figure 12 illustrates the path of propagation of the crack following the eutectic cell boundaries. This obser-

vation is consistent with the expected presence of additional oxide bifilms at these locations. The oxide films are pushed by the growing solid phase, thus finally concentrating in grain boundaries and cell boundaries, providing these regions with varying quantities of pre-existing cracks depending on the cleanness of the alloy. Figure 13(d) shows the presence of small cracks even in Li-modified alloy, confirming that the bifilms are not totally deactivated by Li. (In this respect, Sr in Al-Si alloy is significantly more effective.)

The deep etching technique appears to be capable of revealing what appear to be pre-existent microcracks in

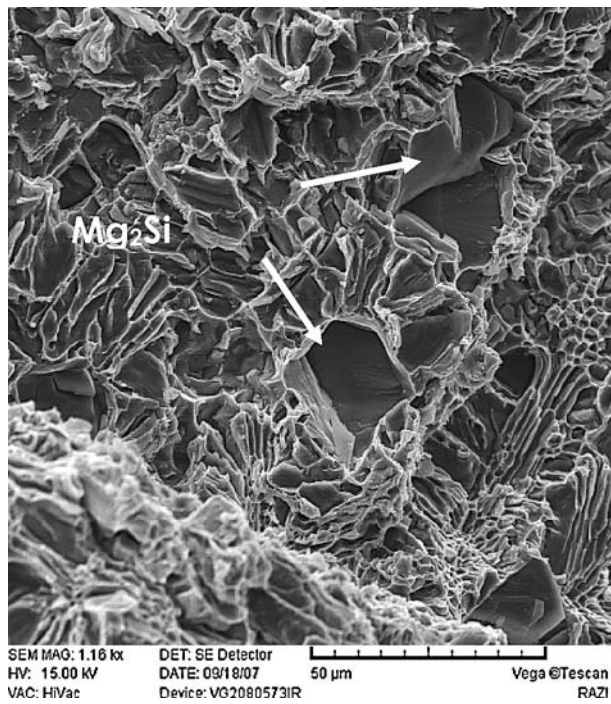


Fig. 10—Typical SEM image of a fracture surface, the upper arrow indicating an Al-Mg<sub>2</sub>Si particle that appears to have peeled open from its central bifilm crack.

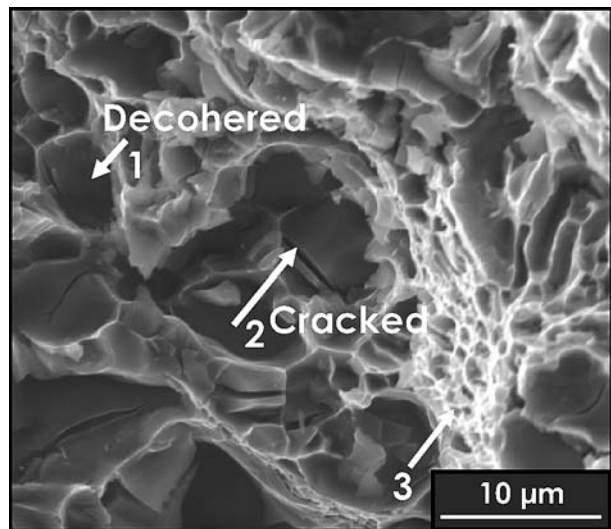


Fig. 11—Cracked and decohered particles in an unmodified 3-mm section.

primary Mg<sub>2</sub>Si particles (Figure 3(a)). Figure 10 exhibits a typical fracture surface of unmodified Al-Mg<sub>2</sub>Si composite, which is composed of large facets, suggesting a brittle mode of failure. The fracture planes of almost all coarse Mg<sub>2</sub>Si particles exhibit what appear to be clear cleavage creating a rapid fracture deriving from their apparent intrinsic brittleness, but more likely as a result of their precracked structure; the appearance of cleavage results from the growth of the faceted intermetallic on a favored interfacial oxide plane, and so is to be expected

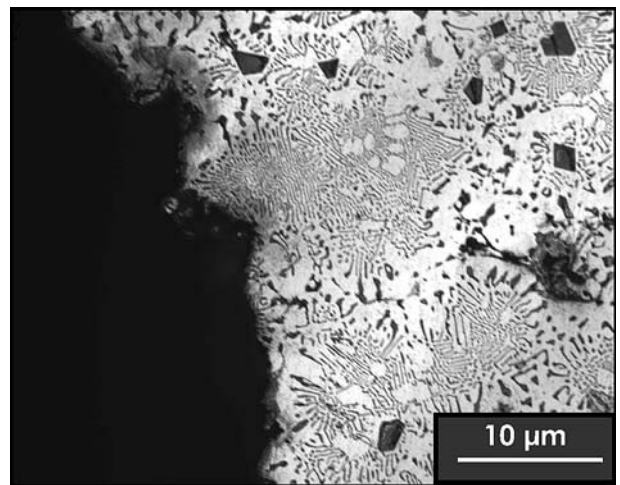


Fig. 12—Optical micrograph showing a side view of the crack propagation path along eutectic cell boundaries.

to be crystallographically flat, and possibly exhibit a preferred intermetallic plane. (It should be noted that some intermetallics with cubic symmetry have such small variations in interfacial energy that no particular planes are necessarily selected. An instance is the alpha-Fe phase in Al-Si alloys<sup>[16]</sup> that consequently grows around the convoluted bifilm, freezing it in place without causing it to straighten, thus improving properties when contrasted with the straightening action of the beta-Fe phase.)

On fracture surfaces of typical MMCs, two major phenomena are well known in the literature: particle decohesion and particle fracture.<sup>[25]</sup> Both phenomena are observed in this study (Figure 11). In terms of the bifilm concept, a particle will exhibit a central crack if the intermetallic forms on both surfaces of the bifilm, and so is likely to crack through its center. If, however, the particle has formed on only one surface of the bifilm, it is likely to appear to decohere from the matrix when subjected to a tensile stress (since in a sense it was never attached to the matrix across this interface, being always separated by the residual air layer in the doubled-over oxide film). The study showed that Li-modified specimens had fewer decohered particles, in agreement the reduction in potency of bifilms by Li, and explains the higher ductility of the MMC. In Figure 11, fine dimples, which are rarely observed in these MMC fracture surfaces, are shown with an arrow (3). These features confirm the intrinsic ductility of the matrix.

Some researchers have emphasized the importance of homogeneous particle distributions to improve ductility.<sup>[26,27]</sup> Adding Li has clearly homogenized the structure and changed the clustering behavior of polyhedral primary particles (Figure 2(b)). If precipitated early from the melt as primary phases, they can be pushed into intercellular regions by the advance of the freezing front. Although such pushing is not expected from interfacial energy considerations, it is seen to be easily feasible if oxide bifilms are also present to separate the advancing front from phases that would otherwise be



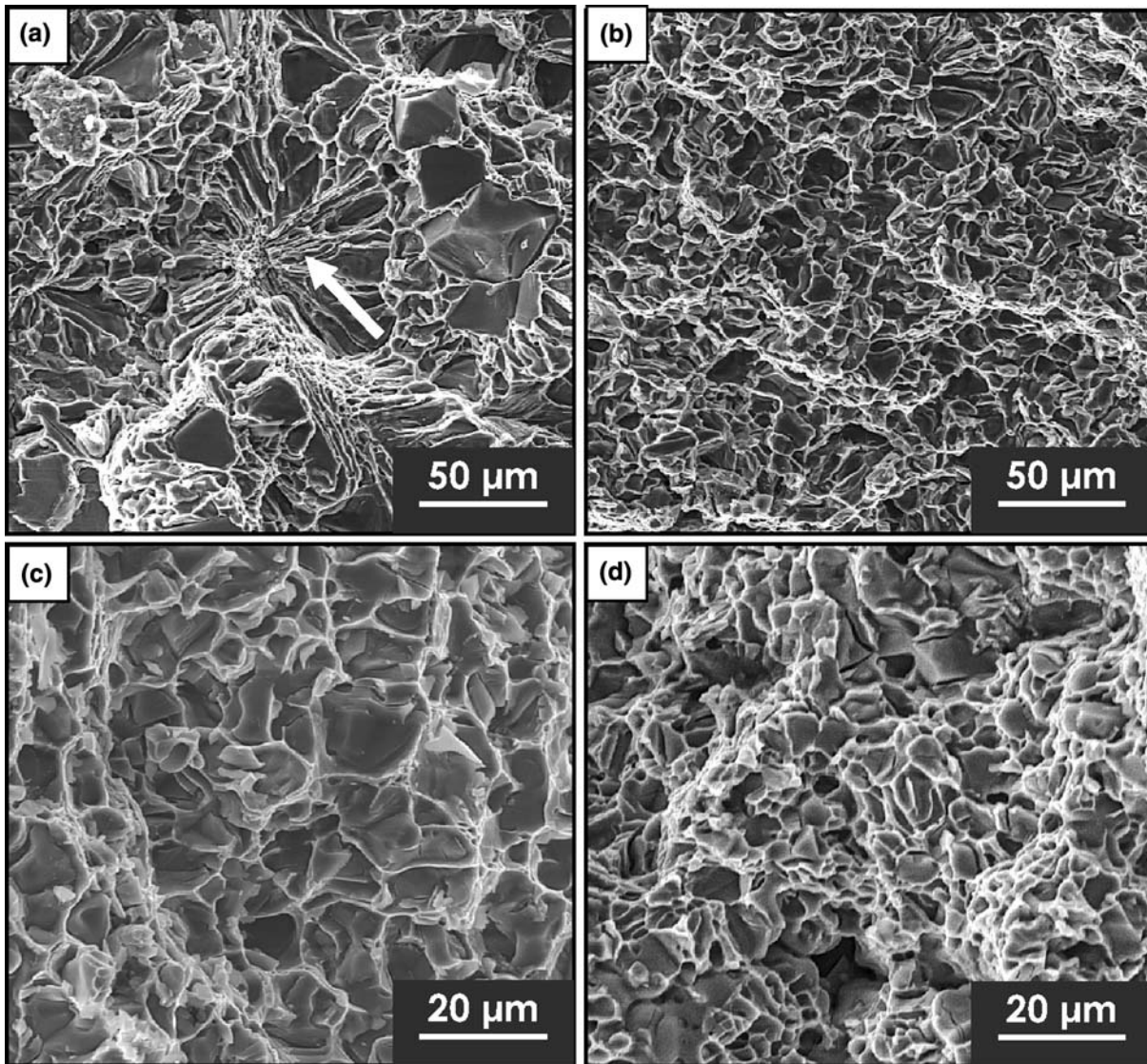


Fig. 13—Fracture surfaces of a 9-mm test bar: (a) unmodified, (b) modified, 3-mm sections at higher magnification, (c) unmodified, and (d) modified.

automatically incorporated. From the microstructures, it is clear that some intermetallics have been incorporated into the eutectic matrix, but others appear to have been pushed. In all cases, any bifilms remain invisible, as is usual and to be expected. After the addition of Li, the suppression of the formation of primary intermetallics (or possibly their much later arrival) reduces this unfavorable pushing action, because the bifilms retain their original compact form and so take a reduced role in the creation of the microstructure.

In Figures 13(a) and (b), the fracture surfaces of an unmodified and Li-modified composite in 9-mm sections are compared. The arrowed region in Figure 13(a) appears to show microcracks along the eutectic flakes inside the eutectic cells. In Figure 13(b), the features are evidently refined; in addition, there is no sign of a similar microcracked region. In Figures 13(c) and (d), the fracture surfaces of 3-mm sections in both modified and unmodified states are compared. As seen in

Figures 13(c) and (d), the convergent pattern arrowed in Figure 13(a) is not observed.

Our observations in this study are in general agreement with those by Johannesson and Caceres<sup>[28]</sup> who added 1 pct Si to an Al-5 pct Mg alloy. They discovered that the elongation to failure fell from around 15 to 3 pct mainly because of the presence of “brittle Mg<sub>2</sub>Si particles.”

The stress-strain curves of the Li-modified alloy exhibit a serrated yielding behavior (Figure 14) reflecting the pinning, and erratic sudden release, of lattice dislocations from solute atom or vacancy atmospheres. Portevin and Le Chatelier originally observed this behavior in Al-Mg alloys arising as a result of dislocation pinning by Mg atoms.<sup>[29,30]</sup>

In the case of this alloy, various possibilities arise.

- (1) It may be that Mg in solid solution in the Al is acting as the pinning solute as in Portevin and Le

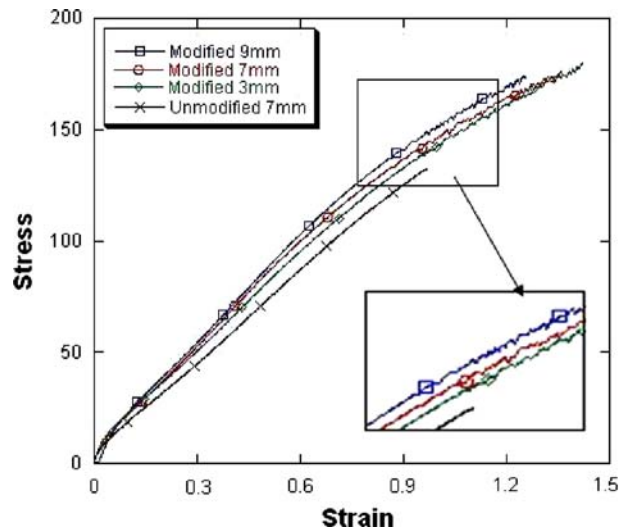


Fig. 14—Serration behavior observed in Li-modified tensile results.

Chateliers' work, in which case (a) the Li addition acts to increase the volume fraction of  $\alpha$ Al phase in the microstructure; although the volume fraction of alpha-Al phase is relatively small, it is completely free to flow plastically, in contrast to (b) the Al phase as part of the eutectic, because the close spacing of the strong intermetallic will significantly reduce this contribution to plastic flow, although, of course, the eutectic volume fraction is high.

- (2) The effect might be related to the direct interaction of Li atoms with dislocations since Li and Mg atomic radii are approximately similar (0.155 and 0.160 nm, respectively). Thus, once again, the Li could act in the Al solid solution either predominantly in (a) the alpha-Al phase of the microstructure or (b) the more constrained Al component as part of the more extensive eutectic phase.

#### IV. CONCLUSIONS

1. Al-15 pct  $Mg_2Si$  composite was prepared by casting direct from the melt. The observed microstructure consists mainly of coarse primary  $Mg_2Si$  particles in a matrix of equiaxed eutectic cells.
2. Adding 0.3 pct Li refined the primary and eutectic cell structures, reducing the average size of primary  $Mg_2Si$  from 30 to  $\sim 6 \mu m$ .
3. Increasing the freezing rate refined the structure to nearly a similar extent.
4. The Li and freezing rate refinement effects were additive.
5. The refined alloy was stronger and more ductile.
6. The benefits of refinement occur principally by a suppression of the unfurling and gradual extension of pre-existing cracks in the liquid (bifilms).
7. Bifilms appear to explain (a) the apparent brittle fracture of  $Mg_2Si$  particles that display apparent

cleavage facets and (b) the apparent decohesion of the particles from the matrix.

8. Large primary  $Mg_2Si$  particles and their clusters appeared to be the favored path for crack propagation, but eutectic cell boundaries were a second common path. Both these paths appeared consistent with their locations for the presence of bifilms; thus, the crack merely follows pre-existing cracks, resulting not from solidification phenomena but from processing phenomena mainly associated with pouring.
9. Evidence was found to confirm the intrinsic strength and ductility of both the matrix and  $Mg_2Si$  particles.
10. Significant additional potential appears to exist for increased properties by improved casting techniques to reduce macroscopic casting defects, particularly in thinner sections.
11. The Li-modified alloy exhibits serrated yielding behavior, which is currently not explained.

#### REFERENCES

1. L. Lu, K.K. Thong, and M. Gupta: *Comp. Sci. Technol.*, 2003, vol. 63, pp. 627–32.
2. M. Mabuchi and K. Higashi: *Acta Mater.*, 1996, vol. 44, p. 4611.
3. E.E. Schmid, K. Von Oldenbrug, and G. Frommeyer: *Z. Metallkd.*, 1990, vol. 81, p. 809.
4. G. Frommeyer, S. Beer, and K. Von Oldenburg: *Z. Metallkd.*, 1994, vol. 85, p. 372.
5. J. Zhang, Z. Fan, Y.Q. Wang, and B.L. Zhou: *J. Mater. Sci. Lett.*, 2000, vol. 19, pp. 1825–28.
6. M.F. Ourfali, I. Todd, and H. Jones: *Metall. Mater. Trans. A*, 2005, vol. 36A, p. 1368.
7. Y.G. Zhao, Q.D. Qin, Y.H. Liang, W. Zhou, and Q.C. Jiang: *J. Mater. Sci.*, 2005, vol. 40, pp. 1831–33.
8. Y.G. Zhao, Q.D. Qin, W. Zhou, and Y.H. Liang: *J. Alloys Compd.*, 2005, vol. 389, pp. L1–L4.
9. J. Zhang, Z. Fan, Y. Wang, and B. Zhou: *J. Mater. Sci. Lett.*, 1999, vol. 18, pp. 783–84.
10. Y.G. Zhao, Q.D. Qin, Y.Q. Zhao, Y.H. Liang, and Q.C. Jiang: *Mater. Lett.*, 2004, vol. 58, pp. 2192–94.
11. J. Zhang, Z. Fan, Y.Q. Wang, and B.L. Zhou: *Scripta Mater.*, 2000, vol. 42, pp. 1101–06.
12. J. Zhang, Z. Fan, Y.Q. Wang, and B.L. Zhou: *Mater. Sci. Eng.*, 2000, vol. A281, pp. 104–12.
13. Q.D. Qin, Y.G. Zhao, W. Zhou, and P.J. Cong: *Mater. Sci. Eng. A*, 2007, vol. 447, pp. 186–91.
14. Y. Flom and R.J. Arsenault: *Acta Mater.*, 1989, vol. 37, p. 2413.
15. J. Campbell: *Castings*, Elsevier, New York, NY, 2003.
16. J. Campbell: *Mater. Sci. Technol.*, 2006, vol. 22 (2), pp. 127–45; No. 8, pp. 999–1008.
17. T. Din, R. Kendrick, and J. Campbell: *Trans. AFS*, 2003, vol. 111, paper no. 03-017.
18. "Standard Methods of Tension Testing Wrought and Cast Aluminum and Magnesium Alloy Products," B557-84, *Annual Book of ASTM Standards*, ASTM, Philadelphia, PA, 1986, vol. 02.2, p. 506.
19. S. Li and S. Zhao: *Mater. Trans. JIM*, 1997, vol. 38, pp. 553–59.
20. W. Kurz and D.J. Fisher: *Fundamentals of Solidification*, 4th edn., Trans Tech Publications Ltd, Switzerland, 1998, p. 12.
21. R.Y. Wang, W.H. Lu, and L.M. Hogan: *J. Cryst. Growth*, 1999, vol. 207, pp. 43–54.
22. R. Hadian and M. Emamy: *Proc. 6th Conf. on Materials Processing, Properties and Performance*, Beijing, Sept. 2007.

23. J.E. Gruzleski and B.M. Closset: *The Treatment of Liquid Aluminum-Silicon Alloys*, American Foundry Society, Des Plaines, IL, 1990.
24. J. Zhang, Y.Q. Wang, and B. Yang: *J. Mater. Res.*, 1999, vol. 14, pp. 68–74.
25. L. Babout: *Acta Mater.*, 2004, vol. 52, pp. 4517–25.
26. J. Segurado and J. LLorca: *Acta Mater.*, 2005, vol. 53, pp. 4931–42.
27. J. LLorca: *Metal-Matrix Composites*, Pergamon Press, Oxford, United Kingdom, 2000, vol. 3, pp. 91–115.
28. B. Johannesson and C.H. Caceres: *Int. J. Cast Met. Res.*, 2004, vol. 17 (2), pp. 94–98.
29. K. Darowicki and J. Orlikowski: *Comput. Mater. Sci.*, 2007, vol. 39, pp. 880–86.
30. R. Hertzberg: *Deformation and Fracture Mechanics*, Wiley, New York, NY, 1983, p. 31.